CORTEX 117 (2019) 311–322

Available online at www.sciencedirect.com

ScienceDirect

Journal homepage: www.elsevier.com/locate/cortex

Research Report

The causal role of the left parietal lobe in facilitation and inhibition of return

E. Martín-Arévalo[*], *J. Lupiáñez, C. Narganes-Pineda, G. Marino, I. Colás and Ana B. Chica*

Department of Experimental Psychology, and Mind, Brain, and Behavior Research Center (CIMCYC), University of Granada, Spain

ARTICLE INFO

Article history:
Received 19 February 2019
Reviewed 30 March 2019
Revised 12 April 2019
Accepted 30 April 2019
Action editor Carlo Umiltà
Published online 18 May 2019

Keywords:
Facilitation
Inhibition of return (IOR)
Superior parietal lobe (SPL)
Superior longitudinal fasciculus (SLF)
Transcranial magnetic stimulation (TMS)

ABSTRACT

Following non-informative peripheral cues, responses are facilitated at the cued compared to the uncued location at short cue-target intervals. This effect reverses at longer intervals, giving rise to Inhibition of Return (IOR). The *integration-segregation* hypothesis (Lupiáñez, 2010) suggests that peripheral cues always produce an onset-detection cost regardless the behavioral cueing effect that is measured – either facilitation or IOR. In the present study, we used transcranial magnetic stimulation (TMS) to investigate the causal contribution of this *detection cost* to performance. We used a cueing paradigm with a target discrimination task that was preceded by a non-informative peripheral cue. The presence-absence of a central intervening event was manipulated. Online TMS to the left superior parietal lobe (compared to an active vertex stimulation) lead to an overall more positive effect (faster responses for cued as compared to uncued trials), by putatively impairing the detection cost contribution to performance. The data revealed a strong association between overall RT and the TMS effect, and also between overall RT and the integrity of the first branch of the left superior longitudinal fascicule. These results have critical implications not only for the open debate about the mechanism/s underlying spatial orienting effects, but also for the growing literature demonstrating that white matter connectivity is crucial for explaining inter-individual behavioral variability.

1. Introduction

The spatial orienting of attention (driven to salient, potentially dangerous, and/or novel events) allows the selection of relevant information in the spatial dimension. Accumulating evidence suggests that the functional and structural properties of fronto-parietal networks underlie this function (Chica, Bartolomeo, & Lupiáñez, 2013; Corbetta, Patel, & Shulman, 2008; Thiebaut de Schotten et al., 2011). When exogenous attention is manipulated by using spatially non-informative

* *Corresponding author.*
E-mail address: emartina@ugr.es (E. Martín-Arévalo).
https://doi.org/10.1016/j.cortex.2019.04.025

peripheral cues (Chica, Martín-Arévalo, Botta, & Lupiáñez, 2014; Posner, 1980), two different behavioral effects can be observed as a function of time: At short cue-target onset asynchronies (CTOAs; ~50–300 msec), reaction times (RTs) are usually shorter for targets appearing at the same location as the peripheral cue (cued locations) as compared to targets presented at the opposite location (uncued locations). At longer CTOAs (longer than ~300 msec, depending on factors such as task demands; see Chica et al., 2014), the behavioral effect reverses, and RTs are shorter for uncued as compared to cued locations (Posner & Cohen, 1984). Posner and colleagues (Posner, Rafal, Choate, & Vaughan, 1985) termed this effect *Inhibition of Return* (IOR), reflecting the theory initially proposed to explain it: IOR would be the consequence of an impaired ability to return attention to a previously attended location (see Klein, 2000, for a review).

Although this *re-orienting hypothesis* about IOR (Klein, 2000; Posner, 1980) has been extensively accepted, it has also been robustly refuted (Berlucchi, 2006; Hu, Samuel, & Chan, 2011; Krüger, MacInnes, & Hunt, 2014; Lupiáñez, Martín-Arévalo, & Chica, 2013; Martín-Arévalo, Chica, & Lupiáñez, 2014). Just to give some examples, IOR can be observed in the absence of previous facilitation (Mele, Savazzi, Marzi, & Berlucchi, 2008; Tassinari, Aglioti, Chelazzi, Peru, & Berlucchi, 1994; Tassinari & Berlucchi, 1995; and therefore, with no evidence of attentional orienting), and IOR can be observed at attended locations (Chica, Lupiáñez, & Bartolomeo, 2006; and therefore, with no evidence of attentional reorienting), or even at fixated locations (Rafal, Davies, & Lauder, 2006). Nowadays, the mechanism/s underlying spatial orienting effects still remain highly debated (see e.g., Lupiáñez, Klein, & Bartolomeo, 2006; Martín-Arévalo, Chica, & Lupiáñez, 2016, for reviews). It has been claimed that spatial orienting effects measured in RT or accuracy data probably reflect the contribution of multiple stages of processing (Berlucchi, 2006; Lupiáñez, 2010; Martín-Arévalo et al., 2016; Taylor & Klein, 2000), although no agreement has yet been reached about which of these stages of processing is/are crucial to the mechanism/s underlying both facilitation and IOR. A new theoretical framework, the *integration-segregation hypothesis* (Lupiáñez, 2010; Lupiáñez et al., 2013), proposes that the orienting of attention produced by peripheral cues is related to two processes: a *spatial selection benefit*, which improves feature discrimination; and a *onset-detection cost*, which impairs target detection. The behavioral cueing effect that is measured – either facilitation or IOR – would result from the net contribution of these processes to performance.

In a previous study (Martín-Arévalo et al., 2014) we used a letter discrimination task preceded by a spatially non-informative peripheral cue, and manipulated the absence or presence of an intervening event during the cue-target period (to favor the appearance of IOR; see e.g., Faust & Balota, 1997; Lupiáñez et al., 2013; Martín-Arévalo, Chica, & Lupiáñez, 2013; Pratt & Fischer, 2002; Prime, Visser, & Ward, 2006). We observed that P1 amplitude was reduced for cued as compared to uncued conditions, and this P1 modulation was independent of the behavioral effect that was measured (either facilitation or IOR). We interpreted (Martín-Arévalo et al., 2014) that P1 modulations might reflect one of the mechanisms underlying spatial orienting effects: the so-called *detection cost* (Lupiáñez, 2010).

1.1. Aims of the present work

In the present study, we used a causal approach to investigate the contribution of the *detection cost* mechanism to exogenous spatial orienting effects by assuming that the P1 component might be reflecting this *detection cost* – an hypothesis based on our previous EEG findings (Martín-Arévalo et al., 2014, 2016). We applied online transcranial magnetic stimulation (TMS) to the left parietal cortex while the participants performed the same task as in Martín-Arévalo et al. (2014). We used source localization analyses (from the EEG data of the previous study; Martín-Arévalo et al., 2014) to identify the neural generator of the P1 component (see Section 2.4). This analysis pointed to a coordinate on the left superior parietal gyrus/lobe (SPL). As in previous studies (Martín-Arévalo et al., 2013, 2014), two groups of participants were compared, one with no intervening event during the cue-target period (intervening event absent group, in which behavioral facilitation was expected), and one with an intervening event during the cue-target period (intervening event present group, in which IOR was expected). Based on previous results (Martín-Arévalo et al., 2014), the CTOAs range used here allows observing both facilitation and IOR in the same paradigm by only manipulating the absence or presence of an intervening event. TMS pulses were applied either to the left SPL or to an active control site (vertex). TMS pulses were target-locked, either at the time in which P1 peaked in our previous study or at a control time-window (see Section 2.5). We hypothesized that left SPL TMS during the P1 peak would reduce the contribution of the *detection cost* to the behavioral effect. In particular, if (as predicted by the *integration-segregation hypothesis*; Lupiáñez, 2010) the *detection cost* were a common process to both facilitation and IOR, which always contributes negatively to performance (increasing RTs in cued as compared to uncued trials), we hypothesized that left SPL TMS might lead to an overall more positive effect (shorter RTs for cued as compared to uncued trials) both when intervening events are present and absent.

Additionally, and given the influence of long-range white matter tracks connecting the parietal and the frontal lobe on cognitive processes (Chica, Thiebaut de Schotten, Bartolomeo, & Paz-Alonso, 2018; Scholz, Klein, Behrens, & Johansen-Berg, 2009; Thiebaut de Schotten et al., 2011), we also analyzed the potential contribution of the integrity of the superior longitudinal fasciculus (SLF) to the results observed. Previous studies have shown influences of the white matter microstructure of the SLF over TMS effects (Buschman & Miller, 2007; Martín-Signes, Pérez-Serrano, & Chica, 2017; Quentin, Chanes, Migliaccio, Valabregue, & Valero-Cabre, 2013; Quentin et al., 2018). Based on these previous results, we expected larger TMS effect on participants with less integrity of the first branch of the left SLF (SLF-I, which overlaps with our stimulation-site; Thiebaut de Schotten et al., 2011). Note that SLF-I (along with SLF-III) has been reliably associated with exogenous spatial orienting both in healthy participants and brain-damaged patients (Bourgeois, Chica, Migliaccio, Thiebaut de Schotten, & Bartolomeo, 2012; Carretie, Rios,

Perianez, Kessel, & Alvarez-Linera, 2012; Doricchi, Thiebaut de Schotten, Tomaiuolo, & Bartolomeo, 2008).

2. Methods

In the result section we report sample size calculation, data exclusion, inclusion/exclusion criteria, whether inclusion/exclusion criteria were established prior to data analysis, all manipulations, and all measures in the study.

2.1. Participants

G*Power 3.1.9.2 was used to determine sample size (Erdfelder, Faul, Buchner, & Lang, 2009) based on our previous EEG findings (Martín-Arévalo et al., 2016). At least sixteen participants were required in each group.

A total of 36 healthy volunteers (all right-handed; 21 women; mean age of 24 years, standard deviations (SD) = 3.3) participated in the study; 18 participants randomly assigned to each group (intervening event absent *vs* intervening event present group). All participants were naïve students from the University of Granada, who signed an informed consent and participated in the experiment for monetary compensation (10 Euros/hour). They were explicitly informed about their freedom to withdraw from the experiment at any time without penalty. Participants had no history of head injury or physical, neurological, or psychiatric illness, and were all tested prior to the experiment for TMS and Magnetic Resonance Imaging (MRI) exclusion criteria (Rossi, Hallett, Rossini, & Pascual-Leone, 2009). Data from two participants in the intervening event absent group were excluded from the final analyses due to a technical error in data acquisition. The experiment was conducted in accordance with the ethical guidelines laid down by the University of Granada, in accordance with the ethical standards of the 1964 Declaration of Helsinki (last update: Seoul, 2008), as part of a larger research project approved by the University of Granada Ethical Committee (175/CEIH/2017).

2.2. Apparatus and stimuli

The experiment was run on a computer (1 GHz Pentium III processor), connected to a 19-inch color VGA monitor (Benq T903, 19″ wide, 1280 × 1024, 60 Hz). E-prime software (Schneider, Eschman, & Zuccolotto, 2002) controlled the presentation of stimuli and the acquisition of data throughout the experiment. All stimuli were drawn in white against a black background. Two placeholder boxes were presented, one on each side of the fixation point (see Fig. 1A). Each box subtended 20 mm in width and 20 mm in height (1.4° × 1.4° of visual angle at a viewing distance of 80 cm). The boxes were positioned 1.8° away from the center of the bottom edges of each placeholder to the center of the screen (fixation point), and positioned .7° above the central fixation along the vertical plane (as measured from the center of the inner lateral edges of each placeholder to the center of the screen). Peripheral cues were created by thickening the outline of one of the two placeholder boxes. The intervening event was created by presenting a smaller box around the fixation point (.7° in width × .7° in height). The target was either the letter "X" or "O" (.14° in width × .14° in height), presented in the center of one of the two placeholder boxes.

2.3. Behavioral procedure

The behavioral procedure (see Fig. 1A) was identical to the one used in Martín-Arévalo et al. (2014). Participants were seated on a comfort TMS robot's armchair (http://www.axilumrobotics.com/en/) at a distance of 80 cm from the screen. Each trial begun with the presentation of the fixation display (containing the fixation point and the two placeholders), with a duration varying randomly between 1000 and 1500 msec. Participants were required to keep their eyes on the fixation point throughout the trials.[1] The peripheral cue was presented for 50 msec in one of the two possible locations with equal probability. In the intervening event present group, the intervening event was presented for 50 msec after a variable (200–300 msec) interval after the peripheral cue. Another fixation display was then presented for a random variable duration of 200–300 msec. In the intervening event absent group, the fixation display was maintained on the screen for the same 50 msec interval, followed by the fixation display, presented for a duration varying randomly between 200 and 300 msec (therefore, keeping a constant CTOA for both groups). The target was displayed for 1200 msec in one of the two peripheral boxes with equal probability. Participants were instructed to discriminate the identity of the letter ("X" or "O") by pressing either the "z" key with their left index finger or the "m" key with their right index finger, with the letter-key assignment being counterbalanced across participants. On 11% of the trials no target was presented (catch trials), and no response was required. The inter-trial interval, in which the screen remained black, lasted for 2000 msec.

2.4. EEG source localization analysis

The EEG source localization analysis was carried out on our previously published EEG data (Martín-Arévalo et al., 2014). The aim of the analysis was to identify the neural generator underlying the P1 component, in order to select the TMS stimulation coordinate. FildTrip Software (Oostenveld, Fries, Maris, & Schoffelen, 2011; http://www.ru.nl/fcdonders/fieldtrip/) and in-house Matlab code were used for this purpose. The localization of brain sources was performed by means of beamforming (Gross et al., 2001; van Veen, van Drongelen, Yuchtman, & Suzuki, 1997). Source localization was performed on a standard MRI in MNI (Montreal Neurological Institute) space provided by the EEGLab toolbox (https://sccn.ucsd.edu/eeglab/), and segmented into 12-mm resolution voxels. The forward

[1] In our previous EEG study (Martín-Arévalo et al., 2014), we used the same behavioral procedure to the one used here, and only 3.2% of trials were excluded due to eye movements. Given the technical complexity of the present TMS experiment, we did not control for eye movements by assuming that participants could properly follow instructions and keep their eyes on the fixation point throughout the trials.

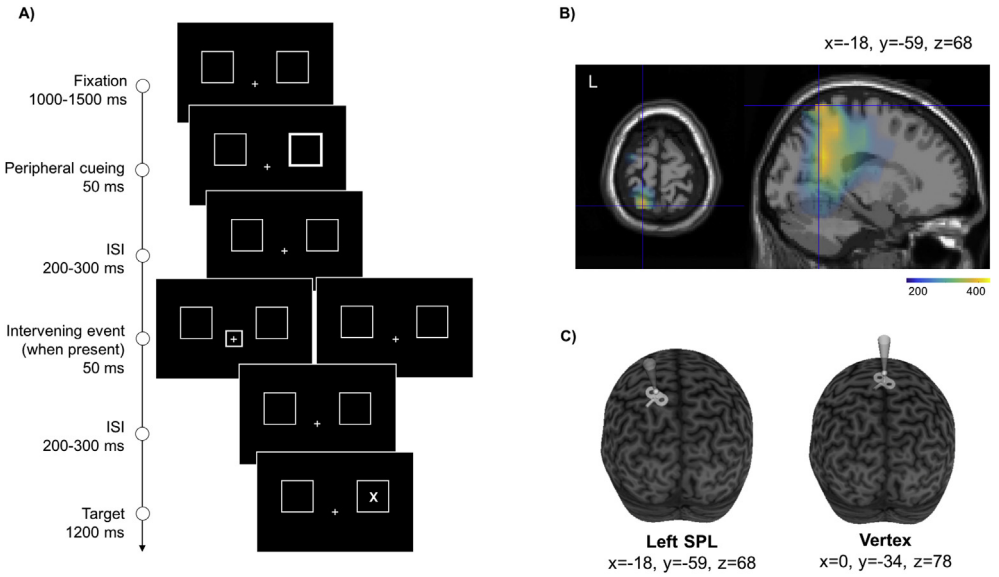

Fig. 1 – A) Sequence de events in a given trial. B) Source localization analysis from our previous EEG data (Martín-Arévalo et al., 2014) pointed to the left superior parietal gyrus/lobe (SPL) as the generator of the P1 component. In the scale, greater values (and/or warmer colors) represent greater brain activity in those areas during the P1 time window (160 msec), expressed as percent relative change respect to the baseline (pre-stimulus) period. L = Left. C) TMS stimulation site based on the source localization analysis (left part) and vertex (right part).

model was computed using a standard boundary element method (BEM) volume conduction model (Oostenveld, Stegeman, Praamstra, & Van Oosterom, 2003) and standard electrode positions. Lead fields were calculated for the 3 possible orientations of each voxel. The EEG signal was band-pass filtered at the frequency of interest (i.e., .1–30 Hz). Then, 60-msec segments corresponding to the time window of interest (i.e., 130–190 msec post-target, the time window showing the largest P1 peak – 160 msec – in our previous study; Martín-Arévalo et al., 2014) were extracted for both cued and uncued conditions, as well as 200 msec from the baseline period (i.e., 200–0 msec pre-target). Intervening event present and absent conditions were collapsed because our previous EEG results demonstrated a main effect of cueing that was independent of the intervening event group (Martín-Arévalo et al., 2014). The activation and baseline segments were concatenated, and we calculated the corresponding covariance matrix, which was used to compute the spatial filter coefficients by means of the linearly constrained minimum variance (LCMV) beamformer (van Veen et al., 1997). We applied regularization (lambda parameter) by adding to the covariance matrix a unit matrix scaled to 10% of the mean across eigenvalues of the covariance matrix. Subsequently, we projected the sensor-level band-pass filtered signal of each trial into the source space through the spatial filter corresponding to the optimally oriented dipole. This orientation was computed for each voxel from the first eigenvector of the covariance matrix between both tangential orientations. The amplitude envelope for each trial (i.e., the absolute value of the Hilbert transform) was averaged across trials and time separately for each cued and uncued condition. To avoid differences in amplitude due to voxels depth, source-level activity was normalized as relative change with respect to the root mean square of the baseline activity for each voxel (Capilla, Belin, & Gross, 2013), and we created mirrored hemi-brain volumes corresponding to both cued and uncued target-related activity. Finally, we averaged the brain activation volumes across participants and identified the voxels exhibiting absolute spatial maxima/minima in the time window showing the largest P1 peak. Following this method, the left superior parietal gyrus/lobe (SPL) was selected as the TMS stimulation site (see Fig. 1B).

2.5. *TMS protocol*

The session began by first determining the hotspot for the first dorsal interosseous (FDI) – defined as the optimum site over primary motor cortex (M1) which evoked the highest contralateral motor evoked potentials (MEP) in the relaxed FDI. Then, we determined the resting motor threshold (rMT), defined as the minimum stimulus intensity which elicits MEPs > 50 μV in five out of ten consecutive trials (Chen, Yung, & Li, 2003; Rossini et al., 2015; Triggs, Calvanio, Macdonell, Cros, & Chiappa, 1994). Electromyography (EMG) and MEPs were recorded from the right FDI by using snap surface electrodes (Natus Neurology). Focal TMS over left M1 was performed with a 70-mm TMS figure-of-eight, connected to a monophasic stimulator (Super Rapid 2, Magstim 2002; Whitland UK) and tangentially held to the scalp at an angle of approximately 45° from the midline (Di Lazzaro et al., 1998).

During the experimental task, the stimulation was administered at 120% of each participant's rMT: mean

intensity = 75% of maximum stimulator output (MSO) in the total sample (SD: 4.1). For the intervening event present group, mean intensity = 75% MSO (SD: 3.4); for the intervening event absent group, mean intensity = 76% MSO (SD: 4.7). On each trial, a burst of two TMS pulses were applied at 50 Hz, with single pulses at 135 and 160 msec after target onset (for the P1 peak condition), and at 175 and 200 msec for the control time window condition. Given the well-known inter- and intra-individual (across trials) peak variability in event-related components we decided to apply a burst of two TMS pulses in order to cover a longer P1 range than exclusively the P1 peak (160 msec ± 3.7 in our previous EEG data).

Scalp coordinates for the stimulation sites were located by using the native space of each participant's T1-weighted anatomical magnetic resonance (MR) scans, acquired at the Brain, Mind, and Behaviour Research Center (CIMCYC), University of Granada. We used a 3-T Siemens magnetization prepared rapid gradient echo, flip-angle = 7, repetition time = 2530 msec, echo time = 2.5 msec, slice thickness = 1 mm, field of view = 256 mm. The TMS coil was controlled by a robotic arm (TMS Robot, Axilum Robotics, http://www.axilumrobotics.com/en/) and a TMS neuronavigation system (Brainsight, Rogue Systems, Montreal, Canada) with the capacity to estimate and track in real time the relative position, orientation, and tilting the coil on the sectional and 3D reconstruction of the participants MRI with a precision of 5 mm. The TMS robot guaranties the accurate stimulation of a given brain region during the experiment, by automatically adjusting its position if a movement larger than 5 mm was detected.

The selected TMS stimulation site (see Fig. 1C), based on the source localization analysis from our previous EEG data (Martín-Arévalo et al., 2014), corresponded to MNI coordinates of $x = -18$, $y = -59$, $z = 68$ (left superior parietal gyrus/lobe; SPL). The control stimulation site was the vertex (MNI coordinates: $x = 0$, $y = -34$, $z = 78$; Heinen et al., 2011), which was not expected to induce any specific behavioral effects based on previous reports (Harris, Benito, Ruzzoli, & Miniussi, 2008; Kalla, Muggleton, Cowey, & Walsh, 2009; Muggleton, Cowey, & Walsh, 2008; Ortiz-Tudela, Martín-Arévalo, Chica, & Lupiañez, 2018).

2.6. Design

The experiment consisted of a four-factor design. Cueing, was manipulated within participants, and had two levels: cued and uncued location trials. Stimulation-time window was manipulated within blocks, and had two levels: P1 peak or control. Stimulation-site was manipulated between blocks, and also had two levels: left SPL and vertex. Intervening event was manipulated between participants, and had two levels: absent versus present. Both the order of stimulation-time window and stimulation site were counterbalanced within participants. Each experiment consisted of 8 practice trials, which were no further analyzed, followed by 576 experimental trials, which were distributed in 2 blocks of 288 trials. Each block corresponded to one stimulation site (left SPL and vertex), and contained 128 cued trials, 128 uncued trials, and 32 catch trials.

2.7. Diffusion tensor imaging (DTI) analysis

DTI analyses were performed following the previously reported procedure (see Supplementary Methods in Thiebaut de Schotten et al., 2011). A total of 70 near-axial slices were acquired on a Siemens 3-T system using a sequence fully optimized for DTI of white matter (based on spherical deconvolution; Dell'Acqua, Simmons, Williams, & Catani, 2013), providing isotropic ($2 \times 2 \times 2$ mm) resolution and coverage of the whole head with a posterior-anterior phase of acquisition (echo time = 88 msec and repetition time = 8400 msec). At each slice location, 6 images were acquired with no diffusion gradient applied and 60 diffusion-weighted images in which gradient directions were uniformly distributed in space. The diffusion weighting was equal to a b-value of 1500 sec/mm^2. In each slice, diffusion-weighted data were simultaneously registered and corrected for subject motion and geometrical distortion adjusting the gradient accordingly (ExploreDTI: http://www.exploredti.com). Then, individual dissections of the tracts were carried out with the software TrackVis (http://www.trackvis.org). The first branch of the SLF (SLF-I) was isolated using a multiple region of interest (ROI) approach. SLF-I is the dorsal-most white matter track linking the superior parietal lobule encompassing the intraparietal sulcus, with the middle and superior frontal gyrus (Thiebaut de Schotten et al., 2011), which overlaps with our stimulation-site (left SPL). Parietal ROIs and frontal ROIs (superior frontal region) were delineated around the white matter. A no-part ROI in the temporal white matter was also used to exclude streamlines of the arcuate fasciculus projecting to the temporal lobe (Rojkova et al., 2016; Thiebaut de Schotten et al., 2011). Finally, the index employed as a surrogate for tract microstructural organization (i.e., mean Hindrance Modulated Orientational Anisotropy or HMOA; Dell'Acqua et al., 2013) was extracted from each dissected tract for both the left and right hemisphere. The mean HMOA is defined as the absolute amplitude of each lobe of the fiber orientation distribution and considered highly sensitive to axonal myelination, fiber diameter, and axonal density (Dell'Acqua et al., 2013).

3. Results

3.1. Behavioral results

Trials in which no responses were recorded or an incorrect response was made were excluded from the RT analysis (.39% of the trials). In addition, trials with correct responses deviating more than 2.5SD above each participant's RT mean were also excluded from the RT analysis (.04% of the trials).

Table 1 shows the mean RT and error rates for each experimental condition and intervening event group. A mixed-design ANOVA was conducted to analyze the mean RTs and error rates. Each ANOVA included stimulation-site (left SPL *vs* vertex), TMS-time window (P1 peak *vs* control), and cueing (cued *vs* uncued trials) as within-participants factors, and intervening event group (absent *vs* present) as a

Table 1 – Mean RTs (in msec) for each condition of cueing, stimulation-site, TMS-time window, and intervening event conditions. Error rates are presented in parentheses.

	Intervening event absent group				Intervening event present group			
	Vertex		Left SPL		Vertex		Left SPL	
	P1 peak	Control	P1 peak	Control	P1 peak	Control	P1 peak	Control
Cued	490 (.05)	493 (.05)	485 (.03)	486 (.03)	498 (.05)	498 (.06)	501 (.04)	503 (.03)
Uncued	503 (.06)	499 (.06)	500 (.03)	498 (.03)	488 (.06)	495 (.05)	497 (.05)	500 (.03)

between-participants factor.[2] Given the final sample size used ($n = 34$), post hoc sensitivity analyses showed that the study (with two groups and eight measurements) was sufficiently powered (≥83%) to detect an effect size ≥ .17.

For the analysis of mean *error rates*, only the main effect of stimulation-site (left SPL and vertex) was significant, $F_{1,32} = 5.21$, MSE = .0061, $p = .0292$, $\eta^2_p = .13$, with fewer errors when left SPL was stimulated as compared to the vertex condition (.04 *vs* .06, respectively). All other main effects or interactions were non-significant (all *ps* > .344; except for stimulation-site × TMS-time window × Group, for which $p = .099$).

For the analysis of the *mean RTs*, only the predicted cueing × intervening event interaction reached significance, $F_{1,32} = 12.61$, MSE = 366, $p = .001$, $\eta^2_p = .28$, showing a significant facilitation effect when the intervening event was absent (mean RT for uncued minus cued trials = 11 msec; planned comparison, $p = .0021$), and a non-significant IOR effect when the intervening event was presented (−5 msec; planned comparison, $p = .112$) (Fig. 2A). All other main effects or interactions were non-significant, all *ps* > .149.

To assess the contribution of the integrity of the left SLF-I to the results, the HMOA index of the left SLF-I was introduced as a covariate in the analysis. Apart from the cueing × intervening event interaction, $F_{1,31} = 15.04$, MSE = 345, $p < .001$, $\eta^2_p = .32$, the covariate effect reached significance, $F_{1,31} = 17.18$, MSE = 42,681, $p < .001$, $\eta^2_p = .36$. Participants with lower left SLF-I HMOA showed longer RTs as compared to participants with higher left SLF-I HMOA. A Pearson correlation (see Fig. 2B) also demonstrated a significant negative correlation between the left SLF-I HMOA and the overall mean RT ($r = -.592$, $p < .001$). The higher the HMOA of the left SLF-I the faster the overall RT. The correlation between the left SLF-I HMOA and the overall RT was significant for both the left SPL and the vertex group ($r = -.579$ and $r = -.583$, respectively; both *ps* < .001). All other main effects or interactions in the ANOVA were non-significant (all *ps* > .100; except for the main effect of cueing, that approached significance, 3 msec; $p = .0789$). Given the proximity of left SLF-I with motor and premotor areas, in order to control that this result was not driven by responses made with the right hand, we performed the same previous ANOVA for each response hand. Both ANOVAs (from right and left response hands) replicated the previous results: cueing × intervening event interaction and the main effect of the covariate.

3.1.1. *Post-hoc analyses*

One interesting (and unexpected) result was the significant relationship between the left SLF-I HMOA and the overall RTs. To explore the contribution of mean RT differences to our data, we repeated the ANOVA with the overall RT as a covariate. Apart from the significant cueing × intervening event group interaction, $F_{1,31} = 13.51$, MSE = 347, $p < .001$, $\eta^2_p = .30$, we observed a significant interaction between stimulated-area and cueing, $F_{1,31} = 7.24$, MSE = 76, $p = .0114$, $\eta^2_p = .18$. Cueing effects were more positive when left SPL was stimulated as compared to the control condition: there was a marginally significant facilitation (5 msec; planned comparison, $p = .072$; −4 msec *vs* 13 msec for the intervening event present and absent group, respectively) when the left SPL was stimulated, and no significant cueing effect when the vertex was stimulated (1 msec; planned comparison, $p = .596$; −7 msec and 9 msec, for the intervening event present and absent group, respectively). The three-way interaction between stimulated-area, cueing, and the overall mean RT covariate was also significant, $F_{1,31} = 9.13$, MSE = 76, $p = .005$, $\eta^2_p = .24$. As can be observed in Fig. 2D, there was a significant correlation between the cueing effect (mean RT for uncued minus cued trials) and the overall mean RT ($r = .375$, $p = .029$) only when left SPL was stimulated. When the vertex was stimulated, this correlation was non-significant ($r = .0245$, $p = .891$). This was also true even when excluding data from 2 participants demonstrating a cueing effect 2.5 SD above each group (left SPL *vs* vertex) mean cueing effect. These results

[2] In the initial analysis, target location (left *vs* right-side) was introduced as a within-participants factor in the ANOVA. Although the main effect of target location reached significance, $F_{1,32} = 7.88$, $p = .008$, $\eta^2_p = .17$, with shorter RTs for right-sided targets as compared to left-sided targets (493 *vs* 499 msec, respectively), this factor demonstrated no further interactions (all *ps* > .187; except for the cueing × target location × intervening event interaction, that approached significance; $p = .074$). Simon congruency (i.e., target presented ipsilaterally or contralaterally to the target response hand) was also introduced as a within-participants factor in the ANOVA. There was a significant interaction between Simon congruency and intervening event, $F_{1,32} = 12.06$, $p = .0015$, $\eta^2_p = .27$, with significantly shorter responses for ipsilateral than contralateral targets only when intervening event was absent (10 msec, $p = .0031$; when intervening event was present, -5 msec; $p = .1045$). We also observed an interaction between Simon congruency and stimulation-site, $F_{1,32} = 12.06$, $p = .0015$, $\eta^2_p = .27$, with significantly shorter responses for ipsilateral than contralateral targets only when vertex was stimulated (7 msec, $p = .0141$; when left SPL was stimulated, 1 msec; $p = .5665$). No other main effects or interactions approached significance (all *ps* > .1337). For the sake of simplicity, and because our main predictions were not related to these two variables, target location and Simon congruency were not included in the final analyses and were not further discussed.

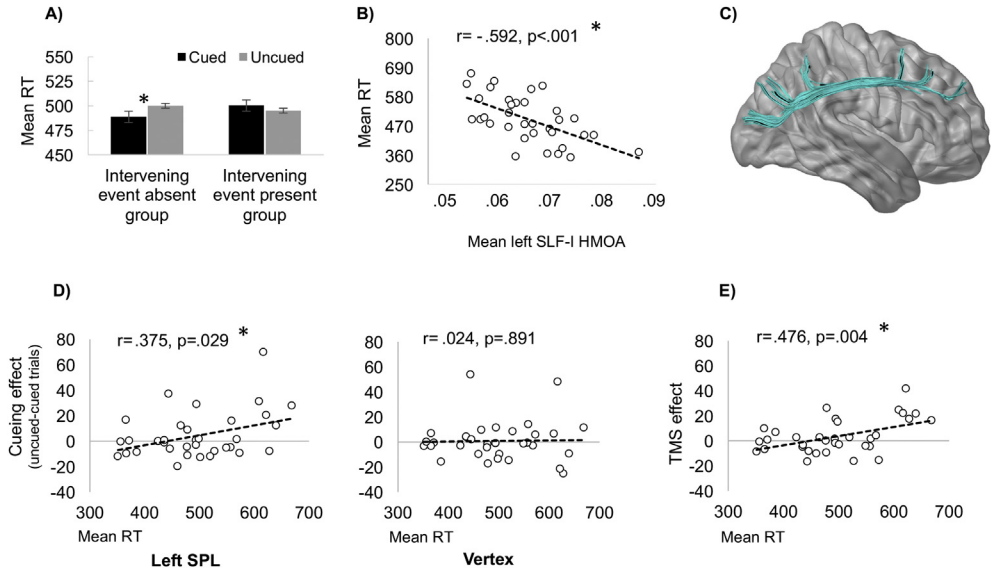

Fig. 2 – A) Mean RTs (in msec) for each experimental condition of cueing, and intervening event. Errors bars represent standard errors of the mean. B) Pearson correlation between the mean overall RT and the mean left SLF-I HMOA. C) Virtual in vivo dissection of the left SLF-I using deterministic tractography. D) Pearson correlation between the mean overall RT and the cueing effect (uncued-cued trials) for both left SPL stimulation (left part) and vertex stimulation (right part). E) Pearson correlation between the mean overall RT and the TMS effect (cueing effect on the SPL-TMS condition minus cueing effect on the vertex–TMS condition). Asterisks represent statistically significant effects.

indicate that applying TMS over the left SPL (with no TMS-time specificity) leads to an overall more positive effect (shorter RTs for cued as compared to uncued trials), especially on those subjects with slower RTs.

Additional analysis considering the TMS effect (cueing effect on the SPL-TMS condition minus cueing effect on the vertex–TMS condition) also revealed a significant correlation between the TMS effect and the overall mean RT ($r = .476$, $p = .004$). As can be observed in Fig. 2E, the slower the overall RT, the more increased the TMS effect. This result again indicates that applying TMS over left SPL leads to an overall more positive effect (faster RTs for cued as compared to uncued trials). All other main effects or interactions were non-significant, all $ps > .1092$.

Finally, in order to better understand the jointed contribution of the SLF-I HMOA and overall RT to the TMS effect observed here, we performed a network analysis (implemented in JASP software: https://jasp-stats.org) with left SLF-I HMOA, overall RT, and the TMS effect. The process was bootstrapped 100 times, using non-parametric bootstrapping. As can be observed in Fig. 3, we observed a positive association (.39) between the overall RT and the TMS effect, and a negative association (−.59) between overall RT and left SLF-I HMOA. Interestingly, the left SLF-I HMOA and TMS effect were not directly associated. This result confirms that it is the overall RT, rather than the left SLF-I HMOA, that correlates with the TMS effect over left SPL. We performed a control analysis using the right SLF-I HMOA, the mean overall RT, and the TMS effect, and we observed no associations among these factors (all values = 0).

In sum, the present data reveal an association between the mean overall RT and the predicted TMS modulation over the left SPL (i.e. leading to more positive or less negative cueing effect), and a remarkable correlation between the mean overall RT and the left SLF-I HMOA. RTs were overall shorter for cued as compared to uncued trials (observing an overall more positive effect) when the left SPL was stimulated (with no TMS-time modulation); an effect putatively related to the interference of the *detection cost* process, which seem to commonly affect both facilitation and IOR.

4. Discussion

The aim of the present study was to investigate the contribution of the *detection cost* to the exogenous cueing effect (Lupiáñez, 2010). We applied online TMS to the left SPL while participants

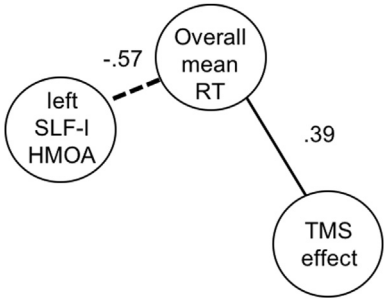

Fig. 3 – Network plot of non-zero edges for main variables in each model (EBIC graphical lasso). Model including left SLF-I HMOA, mean overall RT, and the TMS effect. Thick lines represent positive associations, while dashed lines represent negative associations. No lines represent no associations. The line thickness represents the strength of the association and numbers indicate the weight of the association.

performed a letter discrimination task, preceded by a non-informative peripheral cue (Martín-Arévalo et al., 2013, 2014). The presence-absence of an intervening event was manipulated to observe both facilitation and IOR (Martín-Arévalo et al., 2013).

Behaviorally, we observed a significant behavioral facilitation when no intervening event was presented, and a trend towards IOR when an intervening event was presented (Martín-Arévalo et al., 2013, 2014). These results provide additional empirical support in favor of the effectiveness of an intervening event in producing IOR. Although our results only showed a trend towards IOR, facilitation was significantly abolished when the intervening event was presented (Faust & Balota, 1997; Kingstone & Pratt, 1999; Lupiáñez et al., 2013; Martín-Arévalo et al., 2013; Pratt & Fischer, 2002; Prime et al., 2006; Sapir, Henik, Dobrusin, & Hochman, 2001). It might be argued that the non-significant IOR in the intervening event present group could be problematic. However, we consider that the non-significant IOR do not undermine our conclusions for two main reasons: 1) there was a significant interaction between cueing and intervening event; 2) the intervening event demonstrated no further interactions with other variables (all *ps* > .2365).

More relevant for the main aim of the present study were the results related to the TMS manipulation, which depended on the overall mean RT. Applying TMS over left SPL led to an overall more positive cueing effect (faster RTs for cued as compared to uncued trials), both when the intervening event was present and when it was absent, especially for those subjects with slower RTs. This result, which emerged after post-hoc data exploration, has important implications though. On the one hand, it reveals a very interesting association between the overall RT and the TMS modulation over exogenous orienting effects. The mean overall RT also showed an interesting correlation with the left SLF-I HMOA, which (unexpectedly) seemed not to be directly related to the TMS modulation. We reckon that this result is unrelated to the cueing effect but discloses, however, a tract-specific association between the overall RT and the left SLF-I HMOA. As proposed elsewhere (Chica, Bartolomeo, & Valero-Cabré, 2011; Martín-Signes et al., 2017; Quentin et al., 2013, 2018), inter-individual white matter connectivity might contribute to some extent to variability in TMS effectiveness and by extension to the performance inter-individual inconsistency (Bijsterbosch, Barker, Lee, & Woodruff, 2012). Given that the HMOA index used here is highly sensitive to axonal myelination, fiber diameter, and axonal density (Dell'Acqua et al., 2013) – all these aspects being related to the conduction speed across white matter tracks – we reasoned (based on previous literature; Tuch et al., 2005; Walhovd & Fjell, 2007) that lower conduction speed may lead to slower RTs in the present study. This result fits well with findings wherein individual differences in performance are associated with variations in the white matter characteristics underlying attentional networks (Tuch et al., 2005; Walhovd & Fjell, 2007). This logic also fits with the current data, wherein those participants with high left SLF-I HMOA showed shorter RTs, being probably sheltered from the TMS modulation (see also Martín-Signes et al., 2017).

On the other hand, TMS over left SPL led to an overall more positive cueing effect, which following the *integration-segregation hypothesis* (Lupiáñez, 2010; Lupiáñez et al., 2013), supports the idea of the *detection cost* as a common process contributing to both facilitation and IOR (Lupiáñez, 2010; Lupiáñez et al., 2013). Our proposal is that TMS over left SPL reduced the weight of the negative contributor to performance (*detection cost*), thus leading to an overall more positive effect.

In relation to the role of the left SPL on the present behavioral cueing effects, although there is evidence supporting the right-hemispheric dominance related to exogenous orienting in both the healthy brain (Chica et al., 2011; Shulman et al., 2009) and brain-damaged patients (Bartolomeo, 2007; Bartolomeo, Thiebaut de Schotten, & Chica, 2012), attentional orienting is thought to be related to the functioning of a bilateral dorsal fronto-parietal network (Chica et al., 2011; Corbetta et al., 2008; Kincade, Abrams, Astafiev, Shulman, & Corbetta, 2005). Accordingly, exogenous attention might depend on a bilateral circuit, perhaps with the right-hemispheric dominance in most, but not all, individuals (Heilman & Van Den Abell, 1980; Kinsbourne, 1977). For example, by using offline repetitive TMS (rTMS) in detection tasks, a similar pattern of result has been reported by applying rTMS either over right or left PPC (Hilgetag, Theoret, & Pascual-Leone, 2001; Pascual-Leone et al., 1994). This result is also in line with data from split-brain patients, still showing IOR for right-sided targets when stimulation was presented to the left hemisphere (Berlucchi, Aglioti, & Tassinari, 1997). The right-dominance fits well, however, with previous outcomes wherein TMS (rTMS and single/paired-pulse TMS) over the right PPC (but not the left) has proven to disrupt both manual IOR (Bourgeois, Chica, Valero-Cabre, & Bartolomeo, 2013; Bourgeois, Chica, Valero-Cabré, & Bartolomeo, 2013; see also Chica et al., 2011) and IOR spatial remapping (van Koningsbruggen, Gabay, Sapir, Henik, & Rafal, 2010). Therefore, although some studies have shown a right-lateralized network for the exogenous cueing effect, others have not. Two aspects are important to consider: (i) the right (or left) stimulated-areas in previous studies do not match with the one stimulated here. While previous studies have always stimulated more inferior areas over the intraparietal sulcus or SPL (Bourgeois, Chica, Valero-Cabre, et al., 2013; Du, Chen, & Zhou, 2012; Wu et al., 2016), we stimulated a slightly more superior area over the SPL; and (ii) previous studies showing no TMS effect with left parietal stimulation (Bourgeois, Chica, Valero-Cabre, et al., 2013; Du et al., 2012) did not include individual differences in white matter or RT in their analyses. This was a crucial factor for explaining our results: only those participants with lower left SLF-I HMOA (and slower RTs) showed the TMS modulation over left SPL.

Thus, variables such as the offline rTMS versus online TMS approach, TMS parameters, the stimulated-area (Bolognini & Ro, 2010), and especially the potential contribution of white matter microstructural properties (Martín-Signes et al., 2017; Quentin et al., 2018), can be critical to explain the discrepancies between the previous literature and the results reported here. Thus, taking all these previous variables into account, we consider – as already proposed elsewhere (Chica et al., 2011; see also; Malkinson & Bartolomeo, 2017) – that different parietal sub-regions (either in the left or right hemisphere) along with interindividual differences in the left SLF-I HMOA could differently contribute to exogenous spatial attention.

Finally, we failed at dissociating the TMS effect at the P1 peak as compared to the control time-window. There might be several reasons underlying this lack of temporal specificity: 1) it is likely that participants varied in their P1 peak temporal range, which we did not measured in the present study. 2) The control time-window might have possibly covered a time-window too close to the P1 peak, underlying the TMS-time window indistinctness. 3) Also, the *detection cost* might plausibly be a process that last longer than the P1 peak range – in spite of being potentially reflected in this component as suggested by our previous study (Martín-Arévalo et al., 2014). 4) TMS temporal resolution might depend upon stimulation parameters such as intensity (Bolognini & Ro, 2010). Note that we, however, individually adjusted the stimulation intensity in order to reduce the inter-individual variability in the susceptibility to TMS. Furthermore, dissimilar temporal-windows of TMS disruption (some very transient) throughout different stimulated-areas (Corthout, Uttl, Ziemann, Cowey, & Hallett, 1999; Ro, Breitmeyer, Burton, Singhal, & Lane, 2003) also suggest that TMS differentially disrupts different cortical tissues (Bolognini & Ro, 2010). It is therefore plausible that the TMS parameters and the approach used here may be on the basis of the unsuccessfully distinction between TMS locked to the P1 peak or to a control time-window, and further studies are definitely required to better understand this null result. We have also observed no spatial specificity (target location/visual field) when applying TMS over the left SPL. Although one could expect some spatial asymmetries due to the left SPL stimulation (Kinsbourne, 1977; Schweid, Rushmore, & Valero-Cabre, 2008; Walsh, Ellison, Ashbridge, & Cowey, 1998), this result is in line with other results wherein disrupting (medial) SPL led to impairments in attentional shifting that were independent on the target spatial location (Capotosto et al., 2013; Shulman et al., 2009; Yantis et al., 2002).

In summary, we used a causal approach to show that the TMS influence over left SPL depended on the overall RT, and this overall RT seemed to be modulated by the integrity of the left SLF-I branch. We observed an overall more positive cueing effect when the left SPL was stimulated but only for those subjects with slower RTs (the subjects who also showed the lower left SLF-I HMOA). We hypothesize that TMS over left SPL might have reduced the contribution of the *detection cost* to the behavioral effect, considering the *detection cost* as a common process to both facilitation and IOR. The present results have critical implications not only for the open debate about the mechanism/s underlying the exogenous spatial orienting effects (Lupiáñez, 2010; Lupiáñez et al., 2013), but also for the growing body of literature showing that white matter connectivity is crucial for explaining inter-individual behavioral variability to cognitive processes, performance, and TMS effects (Bijsterbosch et al., 2012; Chica et al., 2018; Martín-Signes et al., 2017; Quentin et al., 2018; Scholz et al., 2009; Thiebaut de Schotten et al., 2011; Walhovd & Fjell, 2007).

Data availability

Readers seeking access to the data and experimental materials might contact the author Elisa Martín-Arévalo (emartina@ugr.es). Data (at raw and summary level) and experimental materials are also available in the Open Science Framework repository (https://osf.io/x8bv9/DOI 10.17605/OSF.IO/X8BV9). No part of the study procedure or analyses was pre-registered prior to the research being conducted.

Open practices

The study in this article earned an Open Materials and Open Data badges for transparent practices. Materials and data for the study are available at https://osf.io/x8bv9/ DOI 10.17605/OSF.IO/X8BV9.

CRediT authorship contribution statement

E. Martín-Arévalo: Conceptualization, Formal analysis, Funding acquisition, Investigation, Methodology, Project administration, Writing - original draft. **J. Lupiáñez:** Conceptualization, Funding acquisition, Writing - original draft, Supervision. **C. Narganes-Pineda:** Methodology, Resources. **G. Marino:** Methodology, Resources. **I. Colás:** Formal analysis. **Ana B. Chica:** Conceptualization, Funding acquisition, Writing - original draft, Project administration, Supervision.

Acknowledgments

EMA was supported by a Juan de la Cierva postdoctoral fellowship from the Spanish Ministry of Economy, Industry, and Competitiveness (IJCI-2015-23204). CNP was supported by a predoctoral fellowship from the FPU program from the Spanish Ministry of Science and Education (FPU16/05056). Research was funded by the Spanish Ministry of Economy and Competitiveness (research projects PSI2017-84926-P to JL; PSI2014-58681-P and PSI2017-88136-P to ABC). The authors would like to thank Almudena Capilla for her help during the EEG source localization analysis.

REFERENCES

Bartolomeo, P. (2007). Visual neglect. *Current Opinion in Neurology, 20*(4), 381–386.

Bartolomeo, P., Thiebaut de Schotten, M., & Chica, A. B. (2012). Brain networks of visuospatial attention and their disruption in visual neglect. *Frontiers in Human Neuroscience, 6*, 110. https://doi.org/10.3389/fnhum.2012.00110.

Berlucchi, G. (2006). Inhibition of return: A phenomenon in search of a mechanism and a better name. *Cognitive Neuropsychology, 23*(7), 1065–1074.

Berlucchi, G., Aglioti, S., & Tassinari, G. (1997). Rightward attentional bias and left hemisphere dominance in a cue-target light detection task in a callosotomy patient. *Neuropsychologia, 35*(7), 941–952.

Bijsterbosch, J. D., Barker, A. T., Lee, K.-H., & Woodruff, P. W. R. (2012). Where does transcranial magnetic stimulation (TMS) stimulate? Modelling of induced field maps for some common cortical and cerebellar targets. *Medical & Biological Engineering & Computing, 50*, 671–681.

Bolognini, N., & Ro, T. (2010). Transcranial magnetic stimulation: Disrupting neural activity to alter and assess brain function. *Journal of Neuroscience, 30*(29), 9647–9650.

Bourgeois, A., Chica, A. B., Migliaccio, R., Thiebaut de Schotten, M., & Bartolomeo, P. (2012). Cortical control of inhibition of return: Evidence from patients with inferior parietal damage and visual neglect. *Neuropsychologia, 50*(5), 800–809. https://doi.org/10.1016/j.neuropsychologia.2012.01.014. S0028-3932(12)00030-9 [pii].

Bourgeois, A., Chica, A. B., Valero-Cabre, A., & Bartolomeo, P. (2013). Cortical control of inhibition of return: Exploring the causal contributions of the left parietal cortex. *Cortex; a Journal Devoted To the Study of the Nervous System and Behavior, 49*(10), 2927–2934.

Bourgeois, A., Chica, A. B., Valero-Cabré, A., & Bartolomeo, P. (2013). Cortical control of inhibition of return: Causal evidence for task-dependent modulations by dorsal and ventral parietal regions. *Cortex; a Journal Devoted To the Study of the Nervous System and Behavior, 49*(8), 2229–2238.

Buschman, T. J., & Miller, E. K. (2007). Top-down versus bottom-up control of attention in the prefrontal and posterior parietal cortices. *Science, 315*(5820), 1860–1862.

Capilla, A., Belin, P., & Gross, J. (2013). The early spatio-temporal correlates and task independence of cerebral voice processing studied with MEG. *Cerebral Cortex, 23*, 1388–1395.

Capotosto, P., Tosoni, A., Spadone, S., Sestieri, C., Perrucci, M. G., Romani, G. L., et al. (2013). Anatomical segregation of visual selection mechanisms in human parietal cortex. *Journal of Neuroscience, 33*, 6225–6229.

Carretie, L., Rios, M., Perianez, J. A., Kessel, D., & Alvarez-Linera, J. (2012). The role of low and high spatial frequencies in exogenous attention to biologically salient stimuli. *PLos One, 7*(5), e37082.

Chen, R., Yung, D., & Li, J. Y. (2003). Organization of ipsilateral excitatory and inhibitory pathways in the human motor cortex. *Journal of Neurophysiology, 89*, 1256–1264.

Chica, A. B., Bartolomeo, P., & Lupiáñez, J. (2013). Two cognitive and neural systems for endogenous and exogenous spatial attention. *Behavioural Brain Research, 15*(237), 107–123.

Chica, A. B., Bartolomeo, P., & Valero-Cabré, A. (2011). Dorsal and ventral parietal contributions to spatial orienting in the human brain. *Journal of Neuroscience, 31*(22), 8143–8149.

Chica, A. B., Lupiáñez, J., & Bartolomeo, P. (2006). Dissociating inhibition of return from the endogenous orienting of spatial attention: Evidence from detection and discrimination tasks. *Cognitive Neuropsychology, 23*(7), 1015–1034.

Chica, A. B., Martín-Arévalo, E., Botta, F., & Lupiáñez, J. (2014). The Posner paradigm: How to design and interpret spatial attention experiments. *Neuroscience and Bio-Behavioural Reviews, 40*, 35–51.

Chica, A. B., Thiebaut de Schotten, M., Bartolomeo, P., & Paz-Alonso, P. M. (2018). White matter microstructure of attentional networks predicts attention and consciousness functional interactions. *Brain Structure & Function, 223*(2), 653–668.

Corbetta, M., Patel, G., & Shulman, G. L. (2008). The reorienting system of the human brain: From environment to theory of mind. *Neuron, 58*(3), 306–324.

Corthout, E., Uttl, B., Ziemann, U., Cowey, A., & Hallett, M. (1999). Two periods of processing in the (circum)striate visual cortex as revealed by transcranial magnetic stimulation. *Neuropsychologia, 37*, 137–145.

Dell'Acqua, F., Simmons, A., Williams, S., & Catani, M. (2013). Can spherical deconvolution provide more information than fiber orientations? Hindrance modulated orientational anisotropy, a true-tract specific index to characterize white matter diffusion. *Human Brain Mapping, 34*, 2464–2483.

Di Lazzaro, V., Restuccia, D., Oliviero, A., Profice, P., Ferrara, L., Insola, A., et al. (1998). Magnetic transcranial stimulation at intensities below active motor threshold activates intracortical inhibitory circuits. *Experimental Brain Research, 119*, 265–268.

Doricchi, F., Thiebaut de Schotten, M., Tomaiuolo, F., & Bartolomeo, P. (2008). White matter (dis)connections and gray matter (dys)functions in visual neglect: Gaining insights into the brain networks of spatial awareness. *Cortex; a Journal Devoted To the Study of the Nervous System and Behavior, 44*(8), 983–995.

Du, X., Chen, L., & Zhou, K. (2012). The role of the left posterior parietal lobule in top-down modulation on space-based attention: A transcranial magnetic stimulation study. *Human Brain Mapping, 33*, 2477–2486.

Erdfelder, E., Faul, F., Buchner, A., & Lang, A. G. (2009). Statistical power analyses using G*Power 3.1: Tests for correlation and regression analyses. *Behavior Research Methods Instruments Computer, 41*(4), 1149–1160.

Faust, M. E., & Balota, D. A. (1997). Inhibition of return and visuospatial attention in healthy older adults and individuals with dementia of the Alzheimer type. *Neuropsychology, 11*(1), 13–29.

Gross, J., Kujala, J., Hamalainen, M., Timmermann, L., Schnitzler, A., & Salmelin, R. (2001). Dynamic imaging of coherent sources: Studying neural interactions in the human brain. *Proceedings of the National Academy of Sciences of the United States of America, 98*, 694–699.

Harris, I. M., Benito, C. T., Ruzzoli, M., & Miniussi, C. (2008). Effects of right parietal transcranial magnetic stimulation on object identification and orientation judgments. *Journal of Cognitive Neuroscience, 20*, 916–926.

Heilman, K. M., & Van Den Abell, T. (1980). Right hemisphere dominance for attention: The mechanism underlying hemispheric asymmetries of inattention (neglect). *Neurology, 30*(3), 327–330.

Heinen, K., Ruff, C. C., Bjoertomt, O., Schenkluhn, B., Bestmann, S., Blankenburg, F., et al. (2011). Concurrent TMS–fMRI reveals dynamic interhemispheric influences of the right parietal cortex during exogenously cued visuospatial attention. *The European Journal of Neuroscience, 33*(5), 991–1000.

Hilgetag, C. C., Theoret, H., & Pascual-Leone, A. (2001). Enhanced visual spatial attention ipsilateral to rTMS-induced 'virtual lesions' of human parietal cortex. *Nature Neuroscience, 4*(9), 953–957.

Hu, F. K., Samuel, A. G., & Chan, A. S. (2011). Eliminating inhibition of return by changing salient non-spatial attributes in a complex environment. *Journal of Experimental Psychology. General, 140*(1), 35–50.

Kalla, R., Muggleton, N. G., Cowey, A., & Walsh, V. (2009). Human dorsolateral prefrontal cortex is involved in visual search for conjunctions but not features: A theta TMS study. *Cortex; a Journal Devoted To the Study of the Nervous System and Behavior, 75*, 1085–1090.

Kincade, J. M., Abrams, R. A., Astafiev, S. V., Shulman, G. L., & Corbetta, M. (2005). An event-related functional magnetic resonance imaging study of voluntary and stimulus-driven orienting of attention. *Journal of Neuroscience, 25*(18), 4593–4604.

Kingstone, A., & Pratt, J. (1999). Inhibition of return is composed of attentional and oculomotor processes. *Perception & Psychophysics, 61*(6), 1046–1054.

Kinsbourne, M. (1977). Hemi-neglect and hemisphere rivalry. In E. A. Weinstein, & R. P. Friedland (Eds.), *Hemi-inattention and hemisphere specialization* (Vol. 18, pp. 41–49). New York: Raven Press.

Klein, R. M. (2000). Inhibition of return. *Trends in Cognitive Sciences, 4*(4), 138–147.

van Koningsbruggen, M. G., Gabay, S., Sapir, A., Henik, A., & Rafal, R. D. (2010). Hemispheric asymmetry in the remapping and maintenance of visual saliency maps: A TMS study. *Journal of Cognitive Neuroscience, 22*, 1730–1738.
Krüger, H. M., MacInnes, W. J., & Hunt, A. R. (2014). Perceptual merging contributes to cueing effects. *Journal of Vision, 14*(7), 1–12.
Lupiáñez, J. (2010). Inhibition of return. In A. C. Nobre, & J. T. Coull (Eds.), *Attention and time* (pp. 17–34). Oxford, UK: Oxford University Press.
Lupiáñez, J., Klein, R. M., & Bartolomeo, P. (2006). Inhibition of return: Twenty years after. *Cognitive Neuropsychology, 23*(7), 1003–1014.
Lupiáñez, J., Martín-Arévalo, E., & Chica, A. B. (2013). Inhibition of return: Attentional disengagement or detection cost? *Psicológica, 34*, 221–252.
Malkinson, T. S., & Bartolomeo, P. (2017). Fronto-parietal organization for response times in inhibition of return: The FORTIOR model. *Cortex; a Journal Devoted To the Study of the Nervous System and Behavior, 102*, 176–192.
Martín-Arévalo, E., Chica, A. B., & Lupiáñez, J. (2013). Task dependent modulation of exogenous attention: Effects of target duration and intervening events. *Attention Perception & Psychophysics, 75*(6), 1148–1160.
Martín-Arévalo, E., Chica, A. B., & Lupiáñez, J. (2014). Electrophysiological modulations of exogenous attention by intervening events. *Brain and Cognition, 85*, 239–250.
Martín-Arévalo, E., Chica, A. B., & Lupiáñez, J. (2016). No single electrophysiological marker for facilitation and inhibition of return: A review. *Behavioural Brain Research, 300*, 1–10.
Martín-Signes, M., Pérez-Serrano, C., & Chica, A. B. (2017). Causal contributions of the SMA to alertness and consciousness interactions. *Cerebral Cortex*, 1–9.
Mele, S., Savazzi, S., Marzi, C. A., & Berlucchi, G. (2008). Reaction time inhibition from subliminal cues: Is it related to inhibition of return? *Neuropsychologia, 46*(3), 810–819.
Muggleton, N. G., Cowey, A., & Walsh, V. (2008). The role of the angular gyrus in visual conjunction search investigated using signal detection analysis and transcranial magnetic stimulation. *Neuropsychologia, 46*, 2198–2202.
Oostenveld, R., Fries, P., Maris, E., & Schoffelen, J. M. (2011). FieldTrip: Open source software for advanced analysis of MEG, EEG, and invasive electrophysiological data. *Computational Intelligence and Neuroscience, 9*.
Oostenveld, R., Stegeman, D. F., Praamstra, P., & Van Oosterom, A. (2003). Brain symmetry and topographic analysis of lateralized event-related potentials. *Clinical Neurophysiology, 114*, 1194–1202.
Ortiz-Tudela, J., Martín-Arévalo, E., Chica, A. B., & Lupiañez, J. (2018). Semantic incongruity attracts attention at a pre-conscious level: Evidence from a TMS study. *Cortex, 102*, 96–106.
Pascual-Leone, A., Gomez-Tortosa, E., Grafman, J., Alway, D., Nichelli, P., & Hallett, M. (1994). Induction of visual extinction by rapid-rate transcranial magnetic stimulation of parietal lobe. *Neurology, 44*(3 Pt 1), 494–498.
Posner, M. I. (1980). Orienting of attention. *Quarterly Journal of Experimental Psychology, 32*, 3–25.
Posner, M. I., & Cohen, Y. (1984). Components of visual orienting. In H. Bouma, & D. Bouwhuis (Eds.), *Attention and performance X* (pp. 531–556). London: Lawrence Erlbaum.
Posner, M. I., Rafal, R. D., Choate, L. S., & Vaughan, J. (1985). Inhibition of return: Neural basis and function. *Cognitive Neuropsychology, 2*, 211–228.
Pratt, J., & Fischer, M. H. (2002). Examining the role of the fixation cue in inhibition of return. *Canadian Journal of Experimental Psychology, 56*(4), 294–301.
Prime, D. J., Visser, T. A., & Ward, L. M. (2006). Reorienting attention and inhibition of return. *Perception & Psychophysics, 68*(8), 1310–1323.
Quentin, R., Chanes, L., Migliaccio, R., Valabregue, R., & Valero-Cabre, A. (2013). Fronto-tectal white matter connectivity mediates facilitatory effects of non-invasive neurostimulation on visual detection. *Neuroimage, 82*, 344–354.
Quentin, R., Frankston, S. E., Vernet, M., Toba, M. N., Bartolomeo, P., Chanes, L., et al. (2018). Visual contrast sensitivity improvement by right frontal high-beta activity is mediated by contrast gain mechanisms and influenced by fronto-parietal white matter microstructure. *Cerebral Cortex, 26*, 2381–2390.
Rafal, R. D., Davies, J., & Lauder, J. (2006). Inhibitory tagging at subsequently fixated locations: Generation of "inhibition of return" without saccade inhibition. *Visual Cognition, 13*(3), 308–323.
Ro, T., Breitmeyer, B., Burton, P., Singhal, N. S., & Lane, D. (2003). Feedback contributions to visual awareness in human occipital cortex. *Current Biology, 13*, 1038–1041.
Rojkova, K., Volle, E., Urbanski, M., Humbert, F., Dell'Acqua, F., & Thiebaut de Schotten, M. (2016). Atlasing the frontal lobe connections and their variability due to age and education: A spherical deconvolution tractography study. *Brain Structure & Function, 221*, 1751–1766.
Rossi, S., Hallett, M., Rossini, P. M., & Pascual-Leone, A. (2009). The safety of TMS consensus group, safety, ethical considerations, and application guidelines for the use of transcranial magnetic stimulation in clinical practice and research. *Clinical Neurophysiology, 120*, 2008–2039.
Rossini, P. M., Burke, D., Chen, R., Cohen, L., Daskalakis, Z., Di Iorio, R., … Ziemann, U. (2015). Non-invasive electrical and magnetic stimulation of the brain, spinal cord, roots and peripheral nerves: Basic principles and procedures for routine clinical and research application. An updated report from an I.F.C.N. Committee. *Clinical Neurophysiology, 126*(6), 1071–1107.
Sapir, A., Henik, A., Dobrusin, M., & Hochman, E. Y. (2001). Attentional asymmetry in schizophrenia: Disengagement and inhibition of return deficits. *Neuropsychology, 15*(3), 361–370.
Schneider, W., Eschman, A., & Zuccolotto, A. (2002). *E-prime user's guide*. Pittsburg: Psychology Software Tools Inc.
Scholz, J., Klein, M. C., Behrens, T. E. J., & Johansen-Berg, H. (2009). Training induces changes in white matter architecture. *Nature Neuroscience, 12*, 1370–1371.
Schweid, L., Rushmore, R. J., & Valero-Cabre, A. (2008). Cathodal transcranial direct current stimulation on posterior parietal cortex disrupts visuo-spatial processing in the contralateral visual field. *Experimental Brain Research, 186*(3), 409–417.
Shulman, G. L., Astafiev, S. V., Franke, D., Pope, D. L., Snyder, A. Z., McAvoy, M. P., et al. (2009). Interaction of stimulus-driven reorienting and expectation in ventral and dorsal frontoparietal and basal ganglia-cortical networks. *Journal of Neuroscience, 29*(14), 4392–4407. https://doi.org/10.1523/JNEUROSCI.5609-08.2009, 29/14/4392 [pii].
Tassinari, G., Aglioti, S., Chelazzi, L., Peru, A., & Berlucchi, G. (1994). Do peripheral non-informative cues induce early facilitation of target detection? *Vision Research, 34*(2), 179–189.
Tassinari, G., & Berlucchi, G. (1995). Covert orienting to non-informative cues: Reaction time studies. *Behavioural Brain Research, 71*, 101–112.
Taylor, T. L., & Klein, R. (2000). Visual and motor effects in inhibition of return. *Journal of Experimental Psychology: Human Perception and Performance, 26*(5), 1639–1656.
Thiebaut de Schotten, M., Dell'Acqua, F., Forkel, S. J., Simmons, A., Vergani, F., Murphy, D. G. M., et al. (2011). A lateralized brain network for visuospatial attention. *Nature Neuroscience, 14*(10), 1245–1246.

Triggs, W. J., Calvanio, R., Macdonell, R. A. L., Cros, D., & Chiappa, K. H. (1994). Physiological motor asymmetry in human handedness: Evidence from transcranial magnetic stimulation. *Brain Research, 636*(2), 270–476.

Tuch, D. S., Salat, D. H., Wisco, J. J., Zaleta, A. K., Hevelone, N. D., & Rosas, H. D. (2005). Choice reaction time performance correlates with diffusion anisotropy in white matter pathways supporting visuospatial attention. *Proceedings of the National Academy of Sciences of the United States of America, 102*(34), 12212–12217.

van Veen, B. D., van Drongelen, W., Yuchtman, M., & Suzuki, A. (1997). Localization of brain electrical activity via linearly constrained minimum variance spatial filtering. *IEEE Transactions on Biomedical Engineering, 44*, 867–880.

Walhovd, K. B., & Fjell, A. M. (2007). White matter volume predicts reaction time instability. *Neuropsychologia, 45*(10), 2277–2284.

Walsh, V., Ellison, A., Ashbridge, E., & Cowey, A. (1998). The role of the parietal cortex in visual attention—hemispheric asymmetries and the effects of learning: A magnetic stimulation study. *Neuropsychologia, 37*(2), 245–251.

Wu, Y., Wang, J., Zhang, Y., Zheng, D., Zhang, J., Rong, M., et al. (2016). The neuroanatomical basis for posterior superior parietal lobule control lateralization of visuospatial attention. *Frontiers in Neuroanatomy*, 10(32). https://doi.org/10.3389/fnana.2016.00032.

Yantis, S., Schwarzbach, J., Serences, J. T., Carlson, R. L., Steinmetz, M. A., Pekar, J. J., et al. (2002). Transient neural activity in human parietal cortex during spatial attention shifts. *Nature Neuroscience, 5*(10), 995–1002.